

MAPAN-JOURNAL Publisher: METROLOGY SOC INDIA , NPL PREMISES, Address: DR K S KRISHNAN MARG, NEW DELHI, INDIA,

ISSN / eISSN:0970-3950 / 0974-9853

Volume 25-Issue 1-(2025)

https://doi-001.org/1025/17604614163953

From Martial Tradition to Microbial Modulation: Xingyi Quan Reprograms

Gut-Lung Axis for Enhanced Pulmonary Immunity in Aging Adults (A) Check for updates

Hong Wang, Wenging Wang, Huifang Meng, Xiaolong Shi, Rong Li,

Xiaoyan Du, Guodong Zhang, Yanli Xie, Xiaomei Liu*,

Shanxi Key Laboratory for Modernization of TCVM, College of Veterinary Medicine, Department of Sports, Shanxi Agricultural University, Taigu, Shanxi, China; Shanxi

Agricultural University, Taigu, Shanxi, China

Xingyi Quan Training Department, Shanxi Jiuzhou Xingyi Quan Research Institute, Taigu, Shanxi, China;

hanximama1125@126.com* HongW SXAU@163.com wwq89268@163.com 87534685@qq.com 18335462901@163.com liliu990316@163.com 1695128189@qq.com 610089513@gg.com 710015244@gg.com

Department of Sports, Jinzhong College of Information, Taigu, Shanxi, China

Department of Sports, Shanxi Agricultural University, Taigu, Shanxi, China* School of Physical Education, Northeast Normal University, Changchun, Jilin, China

Abstract

Purpose: Although the gut-lung axis crucially modulates respiratory health, the microbiota-metabolite-immune outcomes of traditional mind-body practices remain unclear. We investigated the effects of Xingyi Quan, which involves unique diaphragmatic breathing patterns, on pulmonary function via gut microbiota reprogramming.

Methods: Pulmonary function tests, flow cytometry, 16S rDNA sequencing, and untargeted metabolomics were conducted on 26 long-term Xingyi Quan practitioners (63.7–65.0 years old) and 14 sedentary controls.

Results: Practitioners had significantly higher forced expiratory volume in 1 s (FEV1), forced vital capacity (FVC), FEV1/FVC%, CD4+ T-cell frequency, and antiinflammatory cytokine levels, but lower pro-inflammatory cytokine levels than controls. Their gut microbiota was enriched in butyrate-producing genera and depleted in pathobionts, with elevated α -diversity. Practitioners showed 79 differentially abundant metabolites, including pantothenic acid and 3-hydroxybutyric acid, which were enriched in vitamin metabolism and NLR family pyrin domain containing 3 inflammasome regulation pathways. We also found exercise-specific microbial-immune interactions: Bacteroides abundance positively correlated with CD4+ T-cell frequency, while Dorea abundance inversely correlated with interleukin-17A levels.

Conclusions: Xingyi Quan likely improves pulmonary homeostasis by coordinating the microbiota-metabolite-immune crosstalk. We provide mechanistic insight into traditional exercise as a non-pharmacological intervention against age-related respiratory decline..

Keywords: gut microbiota–immunometabolic crosstalk; traditional mind–body exercise; SCFA metabolism

Funding

This work was supported by the Fundamental Research Program of Shanxi Province under Grant 20210302124408; Special Topics for Academic Recovery at Shanxi Agricultural University under Grant 2020xshf44; and National Natural Science Foundation of China Regional Fund Program under Grant 32360217.

Introduction

Respiratory diseases are among the leading global health challenges today, where immune dysregulation is central to their pathogenesis [1-4]. Individuals with chronic lung disorders, such as asthma, chronic obstructive pulmonary disease (COPD), and cystic fibrosis, exhibit not only airway dysbiosis but also components of gastrointestinal perturbation [5-8]. Recent advances in microbial sequencing technologies have revolutionized our understanding of lung—microbiota dynamics, revealing that chronic respiratory exacerbations are characterized not by a lack of microbial diversity, but by compositional shifts or dysbiosis, such as reduced Bacteroidetes populations[9]. A classic example explains COPD exacerbations: the overwhelming domination of Proteobacteria occurs in conjunction with high microbial diversity, which again conflicts with traditional concepts of infectious processes [7,10]. Microbial rebalance

therapies, such as probiotics [11], and low-dose antibiotics like azithromycin have clear clinical effectiveness in reducing exacerbation rates [12,13].

This concept has evolved into the gut-lung axis: a conceptual framework that describes the bidirectional communication between the intestinal and pulmonary ecosystems [14], leading to new treatment opportunities in the context of the gut-lung axis. Indeed, evidence attests to the fact that gut dysbiosis anticipates or accompanies respiratory pathology [15,16]. While mucosa-targeted probiotic interventions modify airway inflammation, probiotic interventions attenuate allergic inflammation through interleukin (IL)-10-dependent pathways [17]. ILC3 trafficking from the gut to the lungs during pneumonia exemplifies the spatial dynamics of this axis [18]. Nonetheless, Nonetheless, several respiratory viral infections, including influenza, can induce gut microbiota (GM) alterations that exacerbate disease severity, leading to gastrointestinal complications and secondary bacterial infections[19,20]. Such mutual interactions thus encourage GM modulation as a strategic target of therapeutic respiratory disease management.

Recent findings have, however, brought to light the aspect of exercise as a powerful modulator of respiratory immunity through multi-organ crosstalk, importantly through the gut–lung axis [21,22]. Moderate-intensity exercise spares the upper respiratory tract antiviral defenses [23] while also enhancing GM diversity that will control the balance within T helper 17 cells/regulatory T cells—a key determinant of mucosal immunity [24]. Mechanistically, exercise-induced increases in the short chain fatty acid (SCFA)-producing taxa (e.g., *Lactobacillus, Bifidobacterium*) enhance gut barrier function and suppress nuclear factor kappa B (NF-κB)-mediated pulmonary inflammation. Clinical correlations are evident in patients with COPD exhibiting reduced fecal butyrate levels concomitant with accelerated lung function decline [25]. Notably, structured aerobic training improves pulmonary function indices (e.g., 7.2% forced expiratory volume in 1 second [FEV1]/forced vital capacity [FVC] ratio increase in patients with IBS) through microbial β-diversity remodeling [26].

Xingyi Quan's unique reverse abdominal breathing technique—characterized by chest retraction during inhalation and expansion during exhalation—generates rhythmic diaphragmatic compression, which is hypothesized to enhance gut motility through visceral massage. Preliminary investigations confirm cardiopulmonary benefits from sustained Xingyi Quan practice, with 1-year interventions showing 186 mL improvement in vital capacity and 0.73 L/min increase in maximal oxygen uptake

[27] alongside enhanced adolescent fitness metrics, including increased bone mineral density [28]. Exercise emerges as non-pharmacological therapy modulating T-cell balance and gut-lung crosstalk to improve respiratory outcomes, though traditional mind-body practices require systematic validation [3]. Our study aims to provide new evidence that traditional physical and mental exercises are potential modulators of microbial immune networks. In the current study, we found that Xingyi Quan can regulate the "flora-metabolism-immunity" network in older people, and exercise can modulate gut-derived inflammatory signaling by enriching butyrate-producing bacteria and inhibiting pro-inflammatory bacteria and synergize the activation and regulation of Th17 by *Bacteroides*-associated clusters, thereby enhancing the immunomodulatory pathway and improving lung immune homeostasis.

Materials and Methods

Participants

Twenty-six experienced Xingyi Quan practitioners (13 males [mean \pm SD age: 63.7 \pm 2.4 years] and 13 females [65.0 \pm 1.9 years]) were included, all of whom had practiced at least twice per week for the 3 weeks preceding the study. This cohort has been described in depth previously and had maintained their Xingyi Quan activity for much of their adult lives. For comparison, 14 healthy older individuals (7 males [age: 64.1 \pm 2.1 years] and 7 females [age: 63.9 \pm 1.5 years]) who did not perform physical activity regularly were recruited. Following written informed consent, fasting venous blood samples were collected from all participants between 08:00 and 10:00. Participants were excluded if they had an acute infection, chronic illness, or were taking medications that influence immune function. Additionally, all participants were instructed to abstain from vigorous exercise for 24 h before blood collection. Serum samples were maintained at -80° C for T-lymphocyte subsets and cytokine analysis. Blood samples collected in anticoagulant-treated vacutainers were instantly processed for mononuclear cell isolation. All experiments were reviewed and approved by the XXXX Ethics Committee (identification number: XXXX).

Pulmonary Function Tests

Using an integrated pulmonary function testing system (PowerCube®-Body, Vyaire Medica), we measured FEV1, FVC, and their ratio. The experiment was performed as follows: (1) Key pulmonary function indices were systematically recorded. (2) While performing FVC, the subject was instructed to seal the mouth with

the mouthpiece, that the nose would be occluded, and that the breathing was tidal and maximal inhalation followed by a forced expiration to residual volume and returning to normal tidal breathing. (3) The subject established stable breathing through the mouthpiece, then performed a rapid vital capacity inhalation followed immediately by a forced expiratory maneuver to determine FEV1. All spirometry procedures were performed in triplicate with inter-trial variability controlled. To identify suitable trials, the variability of repeated measurements was required to fall within maximum-minimum differences of ≤ 0.15 L for FVC, ≤ 0.15 L for FEV1, and ≤ 0.67 L/s for PEF. Identification of the best trial followed composite score analysis, considering the measurement that gave the best sum of values for FVC and FEV1 while maintaining all quality criteria.

Flow Cytometry Analysis of T-cell Subsets

Blood samples of 3 mL peripheral blood were withdrawn from both the Control Group and Xingyi Quan Group participants in the fasting state and collected into ethylenediaminetetraacetic acid-K2 anticoagulant tubes. Within 4 h post-collection, 50 μ L of whole blood was incubated with 20 μ L of CD3-FITC/CD8-PE/CD45-PerCP/CD4-APC monoclonal antibody cocktail (Cat# 404002, Kuangbo Thomson Biotechnology, China) for 25 min at room temperature (RT) in darkness. Erythrocyte lysis was performed with 1× hypotonic lysis buffer (10 min, RT), followed by two wash cycles in phosphate-buffered saline (PBS) and centrifugation (500 × g, 5 min). Cell pellets were resuspended in 300 μ L sterile PBS and analyzed using a Mindray BriCyte E6 flow cytometer (488 and 640 nm lasers) with standardized voltage settings.

Serum Cytokine Quantification via Immunofluorescence Assay

Fasting venous blood samples were taken from the Control Group and Xingyi Quan Group between 07:00 and 08:00 AM to minimize circadian variation. Prior to analysis, serum samples were thawed at 4 °C overnight and vortexed for homogeneous resuspension. After 30 min clotting at RT, samples were centrifuged $(1,200 \times g, 15 \text{ min})$ to isolate serum, which was then aliquoted into pre-labeled cryotubes and maintained at -80 °C within 2 h post-collection. Before analysis, serum samples were treated as previously mentioned.

Quantification of serum IL-6/10/17A was performed using a commercially available multiplex immunofluorescence assay kit (Cat# 907002, Kuangbo Thomson Biotechnology, Tianjin, China). Experiments strictly followed the manufacturer's

instructions: (1) Lyophilized calibrators were reconstituted with proprietary dilution buffer to generate an 8-point standard curve (2.3–5,000 pg/mL), with sequential dilutions validated for linearity ($R^2 > 0.98$ for all analytes); (2) 20 μ L of serum samples or standards were incubated with capture antibody-coupled fluorescent microspheres and biotinylated detection antibodies; (3) Streptavidin-phycoerythrin (SA-PE) conjugates were added to form detection complexes. Following two wash cycles (500 \times g, 5 min) to remove unbound reagents, fluorescence signals were acquired on a Mindray BriCyte E6 flow cytometer (Shenzhen Mindray Bio-Medical Electronics, China) which has a 488 nm laser and 585/42 nm PE emission filter.

16S rDNA Sequencing and Bioinformatics Analysis

After sacrifice, feces samples were gathered immediately and frozen at -80 °C. Genomic DNA extraction from GM was conducted using the 338F (5'-ACTCCTACTACGGGAGCAG-3') and 806R (5'-GGGACTACTACHVGTWTCTAA T-3') primer pair targeting the bacterial V3-V4 regions, with subsequent amplification via PCR. The amplification mixture (20 µL total volume) containing 10 ng genomic template DNA, 4 µL 5× FastPfu buffer, 2 µL of 2.5 mM dNTPs, 0.8 µL each of forward and reverse primers (5 µM), 0.4 µL FastPfu polymerase, 0.2 µL BSA, and nuclease-free water to adjust volume. Thermal cycling conditions comprised: 95°C initial denaturation (3 min); 27 cycles of 95 °C for 30 s, 55 °C annealing (30 s), 72 °C extension (45 s); final extension at 72 °C (10 min) then 4 °C hold. Amplified products were verified via 2% agarose gel electrophoresis and purified accordingly. Pooled amplicons underwent paired-end sequencing using Illumina platforms (MiSeq PE300/NovaSeq PE250) following manufacturer protocols (Majorbio Bio-Pharm, Shanghai). Herein, we quality-filtered the raw sequences and clustered them into operational taxonomic units (OTUs) at a 97% similarity threshold via Usearch (v7.1). Representative sequences from each OTU were taxonomically classified, enabling comparative analysis of microbial community structure and diversity metrics. α-Diversity indices (Chao1, Shannon) were computed using Mothur (v1.30), with intergroup comparisons performed through Student's t-test.

Metabolite Extraction and LC-MS/MS Analysis

Human plasma samples (100 μ L) were combined with 400 μ L ice-cold methanol/water (4:1, v/v) that contained 0.02 mg/mL L-2-chlorophenylalanine as an internal standard. The proteins were precipitated by 30 s vortex, 40 kHz ultrasonic extraction at 4 °C for 10 min, 30 min incubation at –20 °C, and centrifugation (13,000 methanol).

 \times g, 4 °C, 15 min). The supernatants were filtered through 0.22 μ m PVDF membranes. To prepare quality control (QC) samples, 20 μ L aliquots were pooled from each processed plasma extract.

Chromatographic separation was performed via an ACQUITY UPLC HSS T3 column (100 × 2.1 mm, 1.8 µm; Waters) with mobile phase A (95% H₂O/5% acetonitrile + 0.1% formic acid) and B (47.5% acetonitrile/47.5% isopropanol/5% H₂O + 0.1% formic acid) at 0.40 mL/min. The gradient started at 0% B for 0.5 min, linearly increased to 25% B over 2.5 min, pumped to 100% B over 9 min, held for 4 min, and re-equilibrated to 0% B over 0.1 min. Mass spectrometry detection used positive/negative switching electrospray ionization (m/z 50-1000) with ionization voltages of 5000 V/-4000 V, a declustering voltage of 80 V, nebulizer/auxiliary gas at 50 psi, curtain gas at 30 psi, source temperature at 500 °C, and collision energy at 20-60 eV. The system stability was monitored by a QC sample analysis every ten experimental runs. Raw LC-MS data process was performed in Progenesis QI (Waters) for feature alignment and generated a retention time-m/z-intensity matrix. Data pretreatment included the removal of metabolites detected in fewer than 80% of samples, values below the lower limit of quantification being cohort-specific minima, sumnormalization, and retention time correction using internal standards. Metabolites with >30% relative standard deviation in QC samples or significant batch effects were excluded. Multivariate analyses using log-transformed data were performed using principal component analysis (PCA), OPLS-DA in R (v1.6.2) was used, and the model validity was assessed for 7-fold cross-validation. Metabolite identification was performed by matching accurate masses (±5 ppm) and MS/MS fragments against the Human Metabolome Database (HMDB) and Metlin Database, and further verification was conducted using plasma-specific spectral libraries. Differently, abundant metabolites were established by variable importance in projection (VIP) scores from OPLS-DA > 1 combined with p-values from Welch's t-test < 0.05, verified by multivariate permutation testing (200 iterations).

Statistical Analysis

Statistical analyses were conducted through GraphPad Prism (v8.0, San Diego, CA, USA). Parametric data were analyzed using the Student's t-test with two-tailed calculations, while nonparametric data were assessed using the Kruskal–Wallis test. Statistical significance was set at *P < 0.05, **P < 0.01, and ***P < 0.001. Data are presented as mean \pm standard error. Spearman correlation analysis was performed in R

(v3.1.1) to assess relationships between bacterial taxa, metabolites, and immune parameters.

Results

Analysis of Pulmonary Function and Immune-Inflammatory Balance

The Xingyi Quan group exhibited significantly higher FEV1, FVC, and FEV1/FVC ratio compared to controls (P < 0.05, Figure 1a). The flow cytometry results showcased significant differences in total T-cell frequency in the peripheral blood mononuclear cell fraction between both groups. Healthy sedentary adults exhibited lower T-cell frequency than Xingyi Quan athletes (P < 0.05, Figure 1b, e). Furthermore, CD4+ T-cell proportion was significantly increased in the Xingyi Quan group (P < 0.05, Figure 1c, e), while those of CD8+ T-cells (Figure 1d, e) and the CD4+/CD8+ T-cell ratio showed no significant alteration (Figure 1e). Xingyi Quan exercise can increase the total T-cells and improve the decline of immunity in the older people by regulating the expression of CD4+ cells.

A multiplex immunofluorescence assay revealed significantly lower serum levels of IL-17A (P < 0.01) and IL-6 (P < 0.05) in the Xingyi Quan group compared to controls (Figure 1f). Moreover, IL-10 levels escalated significantly in the model group (P < 0.001, Figure 1f). Collectively, Xingyi Quan's protective effect of immunity in older people may partly attributed to T lymphocyte regulation and inflammatory factors inhibition.

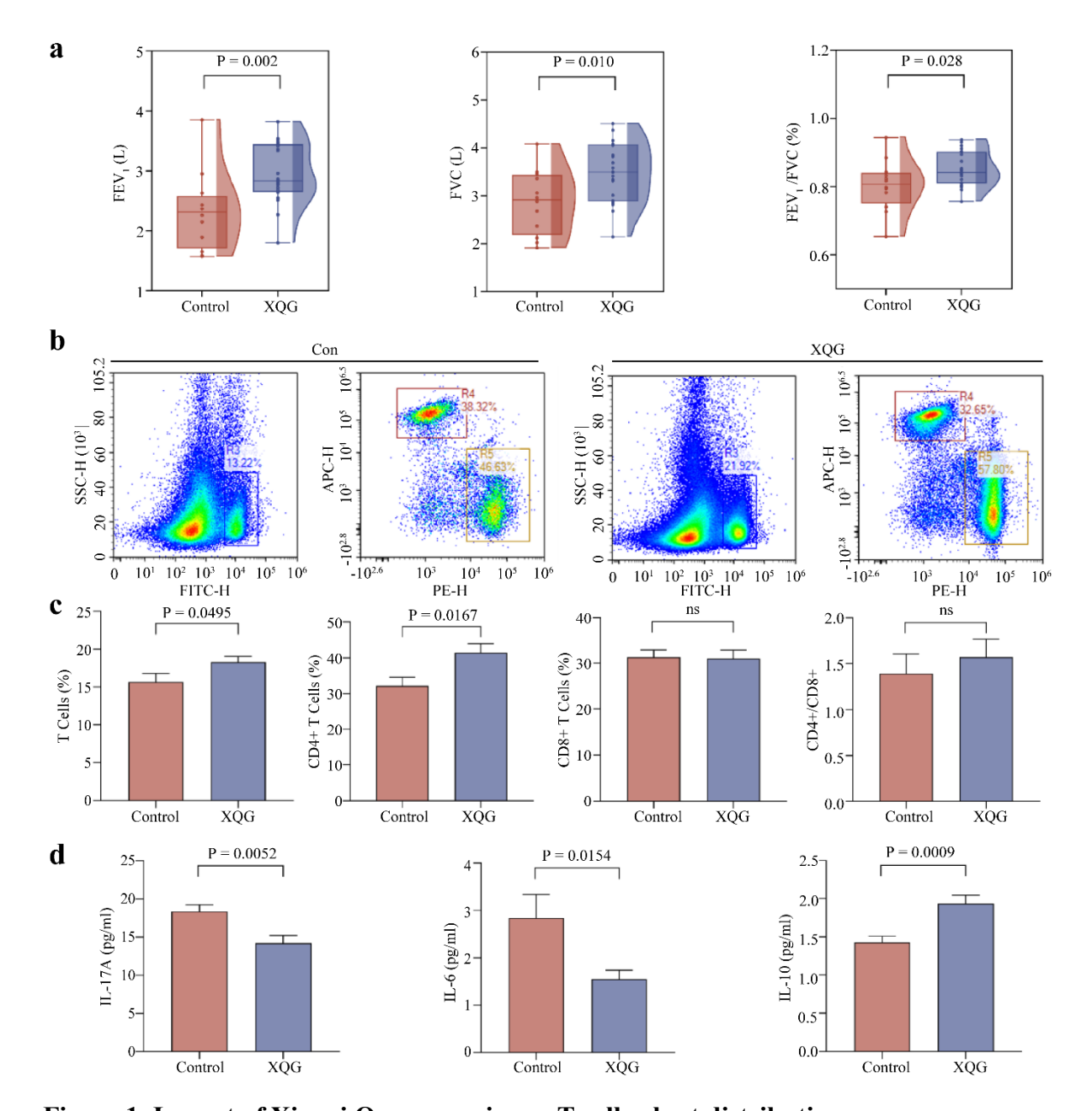


Figure 1. Impact of Xingyi Quan exercise on T-cell subset distribution.

(a) Pulmonary functions of both groups. (b) The representative plots of T-cells were gated by CD3+. R5 and R4 represent the percentage of CD4+ T-cells and CD8+ T-cells, respectively. (c) T-cells in the peripheral blood showing CD3+ T-cell percentage. Further analysis of the CD3+ T-cells showing CD4+ /CD8+ T-cell frequencies and their ratios. (d) Serum IL-17A/ IL-6/ IL-10 levels in both groups. Data interpretation: Mean ± SEM.

Intestinal α - and β -Diversity

Herein, we conducted 16S rDNA gene sequencing on fecal samples from the subjects by first comparing the GM diversity in different groups. Unlike the control, the

α-diversity indices of the GM of Xingyi Quan athletes were significantly higher in the Sobs (P = 0.0088), Chao (P = 0.0033), and Ace indexes (P = 0.0007) (Figure 2a–c), reflecting community richness; the Shannon index (P = 0.0061, Figure 2d) was elevated, and the Simpson index (P = 0.0043, Figure 2e) was lowered reflecting higher diversity of intestinal flora, reflecting the elevated intestinal flora diversity in Xingyi Quan athletes; the Coverage index (P = 0.0290, Figure 2f) was lower than the control. The β-diversity of GM of each group was further analyzed, and the principal coordinate analysis (PCoA) plot showed a trend of all the tested samples forming 2 clusters, one presenting a tightly packed cluster of athletes (Figure 2g, blue dots) and a slightly more dispersed cluster of healthy controls (Figure 2G, red dots). ANOSIM results (Figure 2h) showed a significant structural difference between the group of high-level Xingyi Quan exercisers and the control group were significantly structurally different from each other (P = 0.001, P = 0.369).

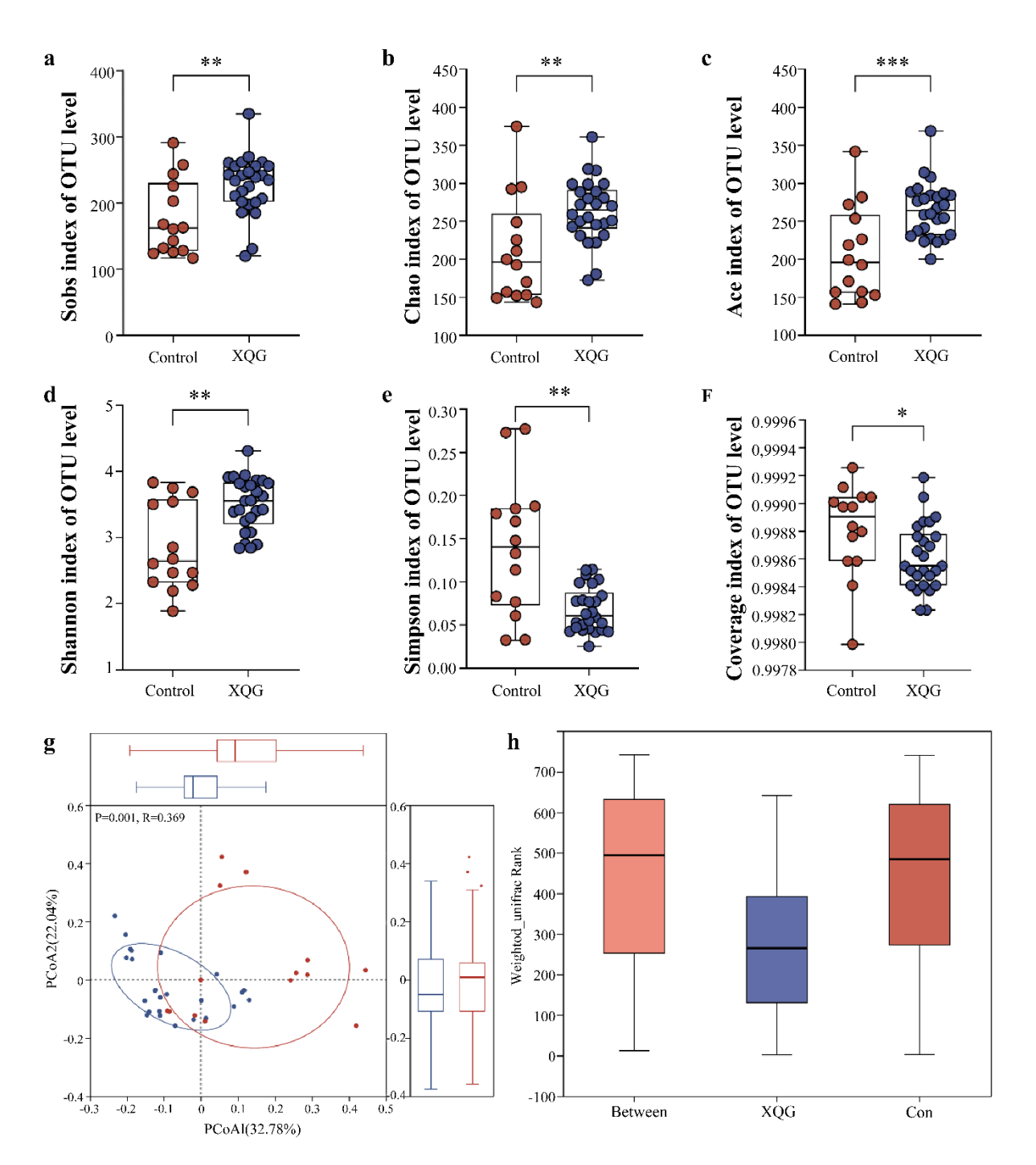


Figure 2. Analysis of fecal microbial diversity.

(a–f) Sobs, Chao 1, Ace, Shannon, Simpson, and Coverage indices: Comparison of α -diversity. (g) PCoA: β -diversity. (h) ANOSIM analysis: Differences between and within both groups. Data interpretation: Mean \pm SD.

GM Alterations and Inflammatory Cytokine Associations

At the phylum level, Firmicutes dominated the gut microbiota, showing the highest abundance, followed by Proteobacteria, Actinobacteria, and Bacteroidota in both groups, all exceeding 5% relative abundance. The XFG group exhibited a distinct

reduction in Bacteroidota abundance and an elevation in that of Actinobacteria compared to controls (Figure 3a). At the genus level, the dominant genera with a relative abundance exciding 2% include Faecalibacterium, Bifidobacterium, Bacteroides, Blautia, Agathobacter, Klebsiella, Subdoligranulum, Escherichia-Shigella, Eubacterium_hallii_group, and Megamonas (Figure 3b). In the control group, Enterococcus, Butyricicoccus,

norank_f_Eubacterium_coprostanoligenes_group, and Ruminococcus_torques_group exhibited positive correlations with IL-6 levels, whereas Klebsiella showed an inverse association.

Blautia and Anaerostipes abundance positively correlated with total T-cell counts, while Megamonas demonstrated a negative correlation with CD8+ T-cells (Figure 3c). In contrast, Xingyi Quan practitioners displayed distinct microbialimmune patterns: Christensenellaceae R-7 group and Ruminococcus torques group maintained positive correlations with IL-6, while Dorea abundance inversely associated with IL-17A levels. Beneficial genera, including Alistipes, Bacteroides, and Faecalibacterium, showed positive associations with both CD4+/CD8+ ratio and CD4+T-cell counts. Conversely, Eubacterium hallii group abundance negatively correlated with CD4+ Tcells, and unclassified f Lachnospiraceae exhibited an inverse relationship with total T-cell counts. Monoglobus and Alistipes demonstrated negative correlations with CD8+ T-cells in the exercise group (Figure 3c).

To analyze the significant differences in GM, we selected the Line Discriminant Analysis (LDA) score exceeding 3 to represent the most enriched species in each group. In terms of GM, unlike the control, *Faecalibacterium*, *Subdoligranulum*, *Eubacterium_hallii_group*, *Anaerostipes*, *Adlercreutzia*, *Lachnospiraceae_NK4A136_group*, *Tyzzerella*, and *UCG-005* were more abundant in the Xingyi Quan group. However, *Escherichia-Shigella*, *Enterobacter*, *Enterococcus*, *Romboutsia*, and *Intestinibacter* exhibited lower relative proportions in the Xingyi Quan group than in the control (Figure 3d).

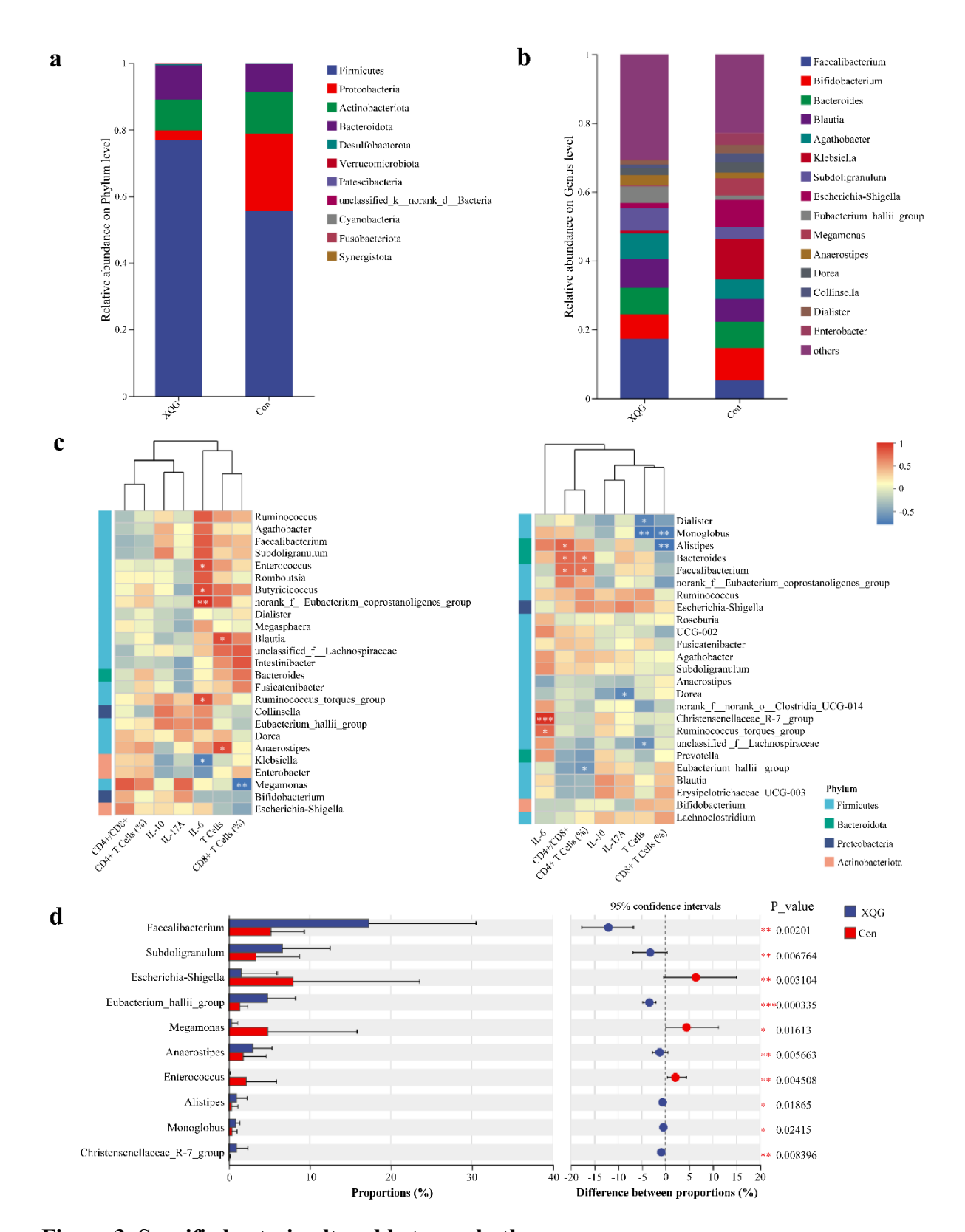


Figure 3. Specific bacteria altered between both groups.

(a) Relative abundance of the most prevalent intestinal bacteria at the phylum and (b) genus levels. (c) Heat map: Hierarchical clustering of Spearman correlation coefficients between fecal bacterial abundance and selected cytokine levels. The photograph on the left depicts the control group, while the photograph on the right shows the XQG group.

(d) Bacteria with significant alternations in the relative abundance in both groups. Data interpretation: Mean \pm SD.

Metabolomics Alterations and Differential Metabolite Profiling

An LC-MS/MS-based untargeted metabolomics analysis identified 523 annotated compounds from primary and secondary mass spectrometry data and library searches (Metlin, HMDB, among others). The results manifested 284 metabolites in the ESI+ model and 239 metabolites in the ESI- model. Kyoto Encyclopedia of Genes and Genomes analysis revealed that these metabolites were significantly enriched in 20 pathways (P < 0.05, Figure 4a) associated with nutrient metabolism, including vitamin digestion and absorption and bile secretion, as well as neuroactive signaling pathways, such as ligand—receptor interactions. The HMDB compounds are categorized into 11 classes in adherence to the Superclass hierarchy, with 133 annotated as Lipids and lipid-like molecules (41.43%), 51 as Organic acids and derivatives (15.89%), 39 as Phenylpropanoids and polyketides (12.15%), followed by Organic oxygen compounds (9.97%) and Organoheterocyclic compounds (8.72%) (Figure 4c).

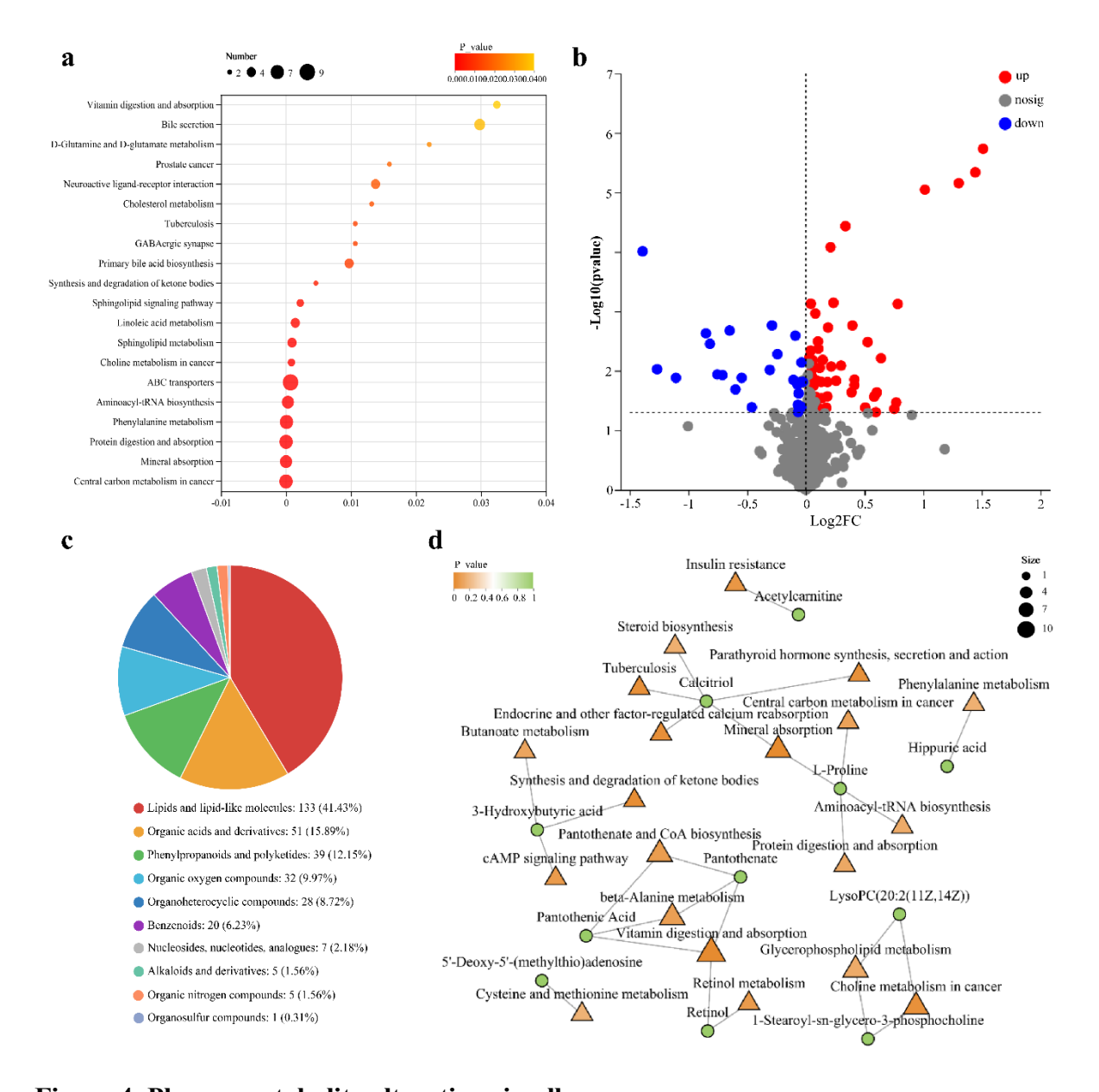


Figure 4. Plasma metabolite alterations in all groups.

(a) KEGG analysis of all metabolites. (b) Difference volcano map of metabolites between both groups. (c) HMDB compounds analysis of all metabolites. (d) Subnetwork analysis of significantly disturbed metabolic pathways.

Metabolites were quantitatively analyzed, with those meeting the criteria of p < 0.05 and VIP > 1 selected for further investigation, identifying 79 differential metabolites in the Xingyi Quan group compared to the Control: 24 downregulated and 55 upregulated (Figure 4b). Among these, 14 metabolites, potentially key biomarkers of Xingyi Quan exercise, were enriched in the top 20 significantly altered pathways between the groups (Figure 5).

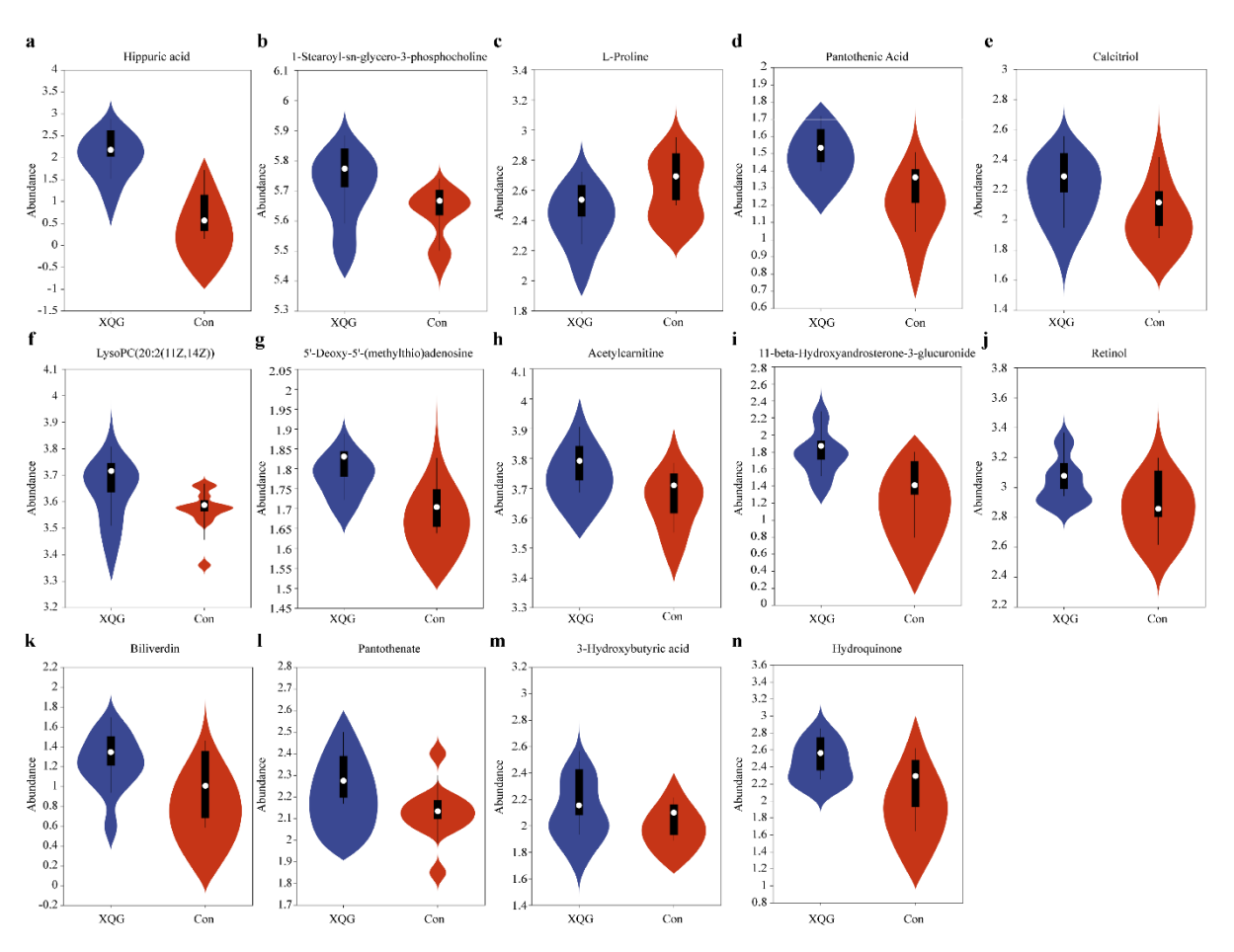


Figure 5. Fourteen key intestinal metabolites associated with Xingyi Quan exercise.

(a) Hippuric acid, (b) 1-stearoyl-sn-glycero-3-phosphocholine, (c) L-proline, (d) pantothenic acid, (e) calcitriol, (f) lysophosphatidylcholine [ysoPC(20:2(11Z,14Z))],

(g) 5'-deoxy-5'-(methylthio)adenosine, (h) acetylcarnitine, (i) 11-beta-hydroxyandrosterone-3-glucuronide, (j) retinol, (k) biliverdin, (l) pantothenate, (m) 3-hydroxybutyric acid, and (n) hydroquinone. Data interpretation: Mean ± SEM.

Discussion

Our findings indicate that Xingyi Quan exercise greatly improves pulmonary function, with increased FEV1, FVC, and FEV1/FVC% values, while modulating immune–inflammatory responses in the elderly residents. The practitioners had higher total T-cell frequency and CD4+ T-cell proportion, lower IL-17A/6 levels, and higher IL-10 levels. The GM analysis indicated greater α -diversity: the Sobs, Chao, Ace, and Shannon indices, and distinct β -diversity clustering for the exercisers. Beneficial genera, such as *Faecalibacterium* and *Subdoligranulum*, were enriched, while opportunistic pathogens, including *Escherichia-Shigella* and *Enterococcus*, were depleted. Seventy-nine differential metabolites were identified through metabolomics

profiling, 79 of which were primarily related to lipid compounds and neuroactive pathway components, with significant enrichment in nutrient metabolism and immune-regulatory pathways. Microbial—immune correlations demonstrated exercise-specific patterns, in which *Faecalibacterium* and *Bacteroides* were positively associated with CD4+ T-cell counts, while *Dorea* abundance was negatively associated with IL-17A levels. Collectively, these multi-omics findings suggest that Xingyi Quan mitigates age-related pulmonary decline via the microbiota—metabolite—immune axis, potentially by enhancing microbial diversity, promoting anti-inflammatory metabolites, and modulating T-lymphocyte activity. Besides, frequency-dominating microbial taxa act in vitamin digestion pathways and signaling molecules to entrain an immunomodulatory way through which this form of exercise protects middle-aged and older people against respiratory decline.

The Five-Fist system (Pi-Beng-Zuan-Pao-Heng) of Xingyi Quan enshrines the organ-meridian correspondence, having the specific association of the Splitting Fist (Pi Quan) with the pulmonary function through the metal element theory, linking the nasal physiology (lung portal) and cutaneous regulation—analogous to modern concepts of the lung–skin axis—through the classical Chinese medical framework. Our preliminary research juxtaposed this certainly putative Qi-mind integration principle of significance in Xingyi Quan [29], fitting with the current considerations concerning multi-tissue microbial-immune interactions along gut-lung-skin axes [1-3,30]. Similar to the immunomodulatory effects observed upon combined exercise training, It has been found by recent research that reduced expression of senescence markers (PD-1 and CD27) and pro-inflammatory cytokines (TNF-α) in PBMCs of patients with diabetes after aerobic-resistance training [30]. Our findings reveal that Xingyi Quan exercise reshapes the GM landscape in elderly practitioners by enriching beneficial taxa (Faecalibacterium, Subdoligranulum, Eubacterium hallii group, Anaerostipes, Christensenellaceae R-7 group) while suppressing pathobionts (Escherichia-Shigella, Megamonas, Enterococcus). These microbiota shifts correlate with improved pulmonary function metrics, likely mediated through anti-inflammatory and immunoregulatory mechanisms along the gut-lung axis.

Xingyi Quan practitioners demonstrate microbial-immune interactions distinct from those of sedentary controls, confirming that the gut-lung axis is modified in a manner specific to exercise. In practitioners, enriched butyrate-producing genera *Faecalibacterium* and *Roseburia* had significant positive correlations with IL-10 and

the CD4+/CD8+ T-cell ratio, whereas associations were generally inversed or absent in those sedentary. This divergence may have resulted from synergistic microbial interactions, whereby *Faecalibacterium* and *Subdoligranulum* act synergistically to produce butyrate and propionate [31,32]. Butyrate appears to strengthen intestinal barrier integrity via its actions on occludin upregulation [33], while the propionate might prime alveolar macrophage efferocytosis through GPR43 signaling [34,35] and establishes a basis for systemic anti-inflammatory effects. Cross-feeding dynamics between Anaerostipes and these butyrogenic taxa further potentiate the SCFA-mediated PPAR-γ activation in lung epithelium by the cross-feeding on SCFAs, in particular, propionic and butyric acids, which the GM produced [36]. The conversion from primary to secondary bile acids by *Eubacterium_hallii_group* might participate in a negative feedback mechanism further inhibiting neutrophilic inflammation in the lungs through the TGR5 receptor [37-39]. These mechanisms likely collaborate to suppress NF-κB and Th17 pathway activation [40], aligning with microbiota-driven immunoregulatory plasticity that promotes pulmonary homeostasis.

In contrast, those associations look dramatically pro-inflammatory in the control group, with a positive relation between *Escherichia-Shigella* relative abundance and IL-6/17A levels. The genus is considered lipopolysaccharide-producing; thus, its exercise-related attenuation would involve reduced systemic inflammation markers, probably via lower Toll-like receptor 4 /NF-κB activation in alveolar macrophages [41]. The same reasoning applies to the reduced acetate overproduction by *Megamonas*, which might reduce NLR family pyrin domain containing 3 (NLRP3) inflammasome priming in bronchial epithelial cells [42]. On the other hand, reduced *Enterococcus* could contribute to the decrease in matrix metalloproteinase-9-mediated tissue degradation implicated in COPD pathogenesis [43]. Overall, Xingyi Quan practice may contain gut-derived inflammatory signaling by reducing pathogen-associated molecular patterns and remodeling the maintenance niche.

Christensenellaceae_R-7_group is a heritable taxon linked with metabolic health [44], thus introducing an additional possible protective mechanism. Although still uncharacterized regarding direct pulmonary impacts, murine modeling suggests metabolites undergirding may inhibit IL-6-driven airway remodeling [45], perhaps accompanying SCFA-mediated immunoregulation. Because some taxa exhibit dual roles, such findings are considered with care: Alistipes-derived indole displays anti-inflammatory potential via aryl hydrocarbon receptor and the suppressor of cytokine

signaling 2 activation [46], while dysregulation may disturb tryptophan metabolism [47], indicating context-dependence in microbial influences. In this regard, *Monoglobus* enrichment probably results from exercise-induced enhancement of mucin barrier function [48] and has nothing to do with any direct pulmonary impact. This underscores the need to disentangle ecological perturbations from physiological consequences. The GM has thus emerged as a significant link in the chain of integrated regulation of SCFA production, bile acid metabolism, and mucosal barrier strengthening, which might explain the putative association of exercise with improvements in pulmonary function.

The synergistic effects of Xingyi Quan's practice on pulmonary function appear to involve coordinated modulation of microbial-derived metabolites that regulate immunometabolic crosstalk. Pantothenic acid emerges as a pivotal immunomodulator through its role as the essential precursor for coenzyme A biosynthesis, with clinical evidence demonstrating dose-dependent enhancement of CD4+ T-cell proliferation and significant elevation of pathogen-specific immunoglobulin A titers in respiratory mucosal surfaces [7]. The ketone body 3-hydroxybutyric acid mediates potent antiinflammatory effects via suppression of NLRP3 inflammasome activation, showing marked reduction in IL-1β secretion from alveolar macrophages under pathological conditions [49-51]. Notably, lysophosphatidylcholine exhibits concentration-dependent duality: physiological levels promote beneficial M2 macrophage polarization through GPR120/STAT3 signaling, while elevated concentrations disrupt pulmonary surfactant homeostasis via LPCAT1-mediated phospholipid remodeling [52,53]. metabolomics landscape suggests that Xingyi Quan-induced microbial shifts may calibrate pulmonary immunity through dynamic regulation of coenzyme metabolism, inflammasome surveillance, and lipid signaling gradients.

However, the study suffers from limited statistical validity due to a small sample size, and the association between flora and immune markers has not been validated for causality. In the future, the spatial dynamics of the gut—lung axis should be elucidated by combining it with a multi-omics analysis of alveolar lavage fluid. In order to clarify the unique benefits of diaphragmatic breathing patterns, randomized controlled trials comparing the specific effects of Xingyi Quan with aerobic/resistance training on lung flora and inflammatory factors are recommended. Through mechanism validation and clinical translation, it is expected that Xingyi Quan will be developed into a precise

exercise intervention program based on colony-immune synergy, providing a non-pharmacological solution to aging-related respiratory decline.

In conclusion, this study reveals that Xingyi Quan improves lung function in the elderly by coordinating intestinal flora remodeling, metabolite regulation, and immune modulation and innovatively constructs the "flora-metabolite-immunity" axis as a mechanistic framework for the association between exercise and respiratory health. Herein, the abundance of butyric acid-producing Faecalibacterium was significantly increased, the pro-inflammatory Escherichia-Shigella was suppressed, and the αdiversity index was significantly increased in the intestinal tracts of the long-term exercisers. Metabolomics identified 79 differential metabolites, of which pantothenic acid and 3-hydroxybutyric acid mediated immune regulation by modulating NLRP3 inflammatory vesicles and vitamin metabolic pathways. Furthermore, colonyimmunity interaction analysis revealed strong positive correlations between Bacteroides abundance and CD4+ T-cell frequency and negative correlations between Dorea and IL-17A, thus revealing potential pathways by which intestinal signals regulate lung immune cells. These findings expand the gut-lung axis theory and confirm that traditional physical and mental exercise can be used as a modulator of multi-organ interactions.

Acknowledgements

Not applicable.

Declaration of Interest

The authors report there are no competing interests to declare.

Data Availability

The data that support the findings of this study are openly available in National Center for Biotechnology Information (NCBI) at https://dataview.ncbi.nlm.nih.gov/object/PRJNA1282331?reviewer=p2ckn7grdks24ua 68g93uiavi1, reference number PRJNA1282331.

References

1. Mazumder MHH, Hussain S. Air-pollution-mediated microbial dysbiosis in health and disease: lung-gut axis and beyond. J Xenobiot. 2024;14:1595–612. https://doi.org/10.3390/jox14040086.

- 2. Singh S, Natalini JG, Segal LN. Lung microbial-host interface through the lens of multi-omics. Mucosal Immunol. 2022;15:837–45. https://doi.org/10.1038/s41385-022-00541-8.
- 3. Bulanda E, Wypych TP. Bypassing the gut–lung axis via microbial metabolites: implications for chronic respiratory diseases. Front Microbiol. 2022;13:857418. https://doi.org/10.3389/fmicb.2022.857418.
- 4. Dickson RP, Martinez FJ, Huffnagle GB. The role of the microbiome in exacerbations of chronic lung diseases. Lancet. 2014;384:691–702. https://doi.org/10.1016/S0140-6736(14)61136-3.
- 5. Roussos A, Koursarakos P, Patsopoulos D, Gerogianni I, Philippou N. Increased prevalence of irritable bowel syndrome in patients with bronchial asthma. Respir Med. 2003;97:75–9. https://doi.org/10.1053/rmed.2001.1409.
- 6. Rutten EPA, Lenaerts K, Buurman WA, Wouters EFM. Disturbed intestinal integrity in patients with COPD: effects of activities of daily living. Chest. 2014;145:245–52. https://doi.org/10.1378/chest.13-0584.
- 7. Bowerman KL, Rehman SF, Vaughan A, Lachner N, Budden KF, Kim RY, et al. Disease-associated gut microbiome and metabolome changes in patients with chronic obstructive pulmonary disease. Nat Commun. 2020;11:5886. https://doi.org/10.1038/s41467-020-19701-0.
- 8. Baral V, Connett G. Acute intestinal obstruction as a presentation of cystic fibrosis in infancy. J Cyst Fibros. 2008;7:277–9. https://doi.org/10.1016/j.jcf.2007.10.005.
- 9. Nielsen S, Needham B, Leach ST, Day AS, Jaffe A, Thomas T, et al. Disrupted progression of the intestinal microbiota with age in children with cystic fibrosis. Sci Rep. 2016;6:24857. https://doi.org/10.1038/srep24857.
- 10. Molyneaux PL, Mallia P, Cox MJ, Footitt J, Willis-Owen SAG, Homola D, et al. Outgrowth of the bacterial airway microbiome after rhinovirus exacerbation of chronic obstructive pulmonary disease. Am J Respir Crit Care Med. 2013;188:1224–31. https://doi.org/10.1164/rccm.201302-0341OC.
- 11. Fujimura KE, Sitarik AR, Havstad S, Lin DL, Levan S, Fadrosh D, et al. Neonatal gut microbiota associates with childhood multisensitized atopy and T cell differentiation. Nat Med. 2016;22:1187–91. https://doi.org/10.1038/nm.4176.
- 12. Alsayed AR, Abed A, Khader HA, Al-Shdifat LMH, Hasoun L, Al-Rshaidat MMD, et al. Molecular accounting and profiling of human respiratory microbial communities: toward precision medicine by targeting the respiratory microbiome for disease

- diagnosis and treatment. Int J Mol Sci. 2023;24:4086. https://doi.org/10.3390/ijms24044086.
- 13. Hiles SA, Mcdonald VM, Guilhermino M, Brusselle GG, Gibson PG. Does maintenance azithromycin reduce asthma exacerbations? An individual participant data meta-analysis. Eur Respir J. 2019;54:1901381. https://doi.org/10.1183/13993003.01381-2019.
- 14. Dang AT, Marsland BJ. Microbes, metabolites, and the gut-lung axis. Mucosal Immunol. 2019;12:843–50. https://doi.org/10.1038/s41385-019-0160-6.
- 15. Ichinohe T, Pang IK, Kumamoto Y, Peaper DR, Ho JH, Murray TS, et al. Microbiota regulates immune defense against respiratory tract influenza A virus infection. Proc Natl Acad Sci U S A. 2011;108:5354–9. https://doi.org/10.1073/pnas.1019378108.
- 16. Russell SL, Gold MJ, Willing BP, Thorson L, McNagny KM, Finlay BB. Perinatal antibiotic treatment affects murine microbiota, immune responses and allergic asthma. Gut Microbes. 2013;4:158–64. https://doi.org/10.4161/gmic.23567.
- 17. Qian G, Jiang W, Zou B, Feng J, Cheng X, Gu J, et al. LPS inactivation by a host lipase allows lung epithelial cell sensitization for allergic asthma. J Exp Med. 2018;215:2397–412. https://doi.org/10.1084/jem.20172225.
- 18. Gray J, Oehrle K, Worthen G, Alenghat T, Whitsett J, Deshmukh H. Intestinal commensal bacteria mediate lung mucosal immunity and promote resistance of newborn mice to infection. Sci Transl Med. 2017;9:eaaf9412. https://doi.org/10.1126/scitranslmed.aaf9412.
- 19. Watzenboeck ML, Drobits B, Zahalka S, Gorki AD, Farhat A, Quattrone F, et al. Lipocalin 2 modulates dendritic cell activity and shapes immunity to influenza in a microbiome dependent manner. PLOS Pathog. 2021;17:e1009487. https://doi.org/10.1371/journal.ppat.1009487.
- 20. Sencio V, Machado MG, Trottein F. The lung-gut axis during viral respiratory infections: the impact of gut dysbiosis on secondary disease outcomes. Mucosal Immunol. 2021;14:296–304. https://doi.org/10.1038/s41385-020-00361-8.
- 21. Kurowski M, Seys S, Bonini M, Del Giacco S, Delgado L, Diamant Z, et al. Physical exercise, immune response, and susceptibility to infections—current knowledge and growing research areas. Allergy. 2022;77:2653–64. https://doi.org/10.1111/all.15328.
- 22. Price OJ, Walsted ES, Bonini M, Brannan JD, Bougault V, Carlsen KH, et al. Diagnosis and management of allergy and respiratory disorders in sport: an EAACI task force position paper. Allergy. 2022;77:2909–23. https://doi.org/10.1111/all.15431.

- 23. Elkhatib SK, Alley J, Jepsen M, Smeins L, Barnes A, Naik S, et al. Exercise duration modulates upper and lower respiratory fluid cellularity, antiviral activity, and lung gene expression. Physiol Rep. 2021;9:e15075. https://doi.org/10.14814/phy2.15075.
- 24. Kim KS. Regulation of T cell repertoires by commensal microbiota. Front Cell Infect Microbiol. 2022;12:1004339. https://doi.org/10.3389/fcimb.2022.1004339.
- 25. Dziewiecka H, Buttar HS, Kasperska A, Ostapiuk-Karolczuk J, Domagalska M, Cichoń J, et al. Physical activity induced alterations of gut microbiota in humans: a systematic review. BMC Sports Sci Med Rehabil. 2022;14:122. https://doi.org/10.1186/s13102-022-00513-2.
- 26. Li M, Sakamoto K, Sato A, Ueno T. Vitamin B5 potentiates respiratory immunity through coenzyme A-dependent bioenergetic rewiring. Front Immunol. 2021;12:694121. https://doi.org/10.3389/fimmu.2021.694121.
- 27. Liang WK, Wang WQ, Li JY. Effects of Xingyiquan on cardiopulmonary indicators in college students. J Shanxi Agric Univ (Soc Sci Ed). 2005;1:83–5.
- 28. Li R, Liu XM, Zhu JL. Effects of practicing Xingyiquan on the physical health of adolescents. Youth Sports. 2016;2:108–9.
- 29. Hao J, Wang W, Wang J. Feasibility analysis of the integration of rural sports culture and Xingyiquan culture: A case study of Taigu County. J Shanxi Agric Univ (Soc Sci Ed). 2013;12:4. https://doi.org/10.13842/j.cnki.issn1671-816x.2013.05.023.
- 30. Brunelli, D. T., Bonfante, I. L. P., Boldrini, V. O., Scolfaro, P. G., Duft, R. G., Mateus, K., Fatori, R. F., Chacon-Mikahil, M. P. T., Farias, A. S., Teixeira, A. M., & Cavaglieri, C. R. (2024). Combined training improves gene expression related to immunosenescence in obese type 2 diabetic individuals. Research Quarterly for Exercise and Sport, 95(3), 730–739. https://doi.org/10.1080/02701367.2023.2299716.
- 31. Sokol H, Pigneur B, Watterlot L, Lakhdari O, Bermúdez-Humarán LG, Gratadoux JJ, et al. Faecalibacterium prausnitzii is an anti-inflammatory commensal bacterium identified by gut microbiota analysis of Crohn disease patients. Proc Natl Acad Sci U S A. 2008;105:16731–6. https://doi.org/10.1073/pnas.0804812105.
- 32. Soto-Martin EC, Warnke I, Farquharson FM, Christodoulou M, Horgan G, Derrien M, et al. Vitamin biosynthesis by human gut butyrate-producing bacteria and cross-feeding in synthetic microbial communities. mBio. 2020;11:e00886-20. https://doi.org/10.1128/mBio.00886-20.
- 33. Li S, Heng X, Guo L, Lessing DJ, Chu W. SCFAs improve disease resistance via modulate gut microbiota, enhance immune response and increase antioxidative capacity

- in the host. Fish Shellfish Immunol. 2022;120:560–8. https://doi.org/10.1016/j.fsi.2021.12.035.
- 34. Zhang Y, Zhang L, Mao L, Fan J, Jiang X, Li N, et al. Intestinal microbiota-derived propionic acid protects against zinc oxide nanoparticle-induced lung injury. Am J Respir Cell Mol Biol. 2022;67:680–94. https://doi.org/10.1165/rcmb.2021-0515OC.
- 35. Feng C, Jin C, Liu K, Yang Z. Microbiota-derived short chain fatty acids: their role and mechanisms in viral infections. Biomed Pharmacother. 2023;160:114414. https://doi.org/10.1016/j.biopha.2023.114414
- 36. den Besten G, van Eunen K, Groen AK, Venema K, Reijngoud DJ, Bakker BM. The role of short-chain fatty acids in the interplay between diet, gut microbiota, and host energy metabolism. J Lipid Res. 2013;54:2325–40. https://doi.org/10.1194/jlr.R036012.
- 37. García-Gavilán JF, Atzeni A, Babio N, Liang L, Belzer C, Vioque J, et al. Effect of 1-year lifestyle intervention with energy-reduced Mediterranean diet and physical activity promotion on the gut metabolome and microbiota: A randomized clinical trial. Am J Clin Nutr. 2024;119:1143–54. https://doi.org/10.1016/j.ajcnut.2024.02.021.
- 38. Liu X, Chen B, You W, Xue S, Qin H, Jiang H. The membrane bile acid receptor TGR5 drives cell growth and migration via activation of the JAK2/STAT3 signaling pathway in non-small cell lung cancer. Cancer Lett. 2018;412:194–207. https://doi.org/10.1016/j.canlet.2017.10.017.
- 39. Wang Y, Liu H, Dong F, Xiao Y, Xiao F, Ge T, et al. Altered gut microbiota and microbial metabolism in children with hepatic glycogen storage disease: A case-control study. Transl Pediatr. 2023;12:572–86. https://doi. https://doi.org/10.21037/tp-22-293.
- 40. Mannion JM, McLoughlin RM, Lalor SJ. The airway microbiome-IL-17 axis: A critical regulator of chronic inflammatory disease. Clin Rev Allergy Immunol. 2023;64:161–78.
- 41. Yamano T, Nedjic J, Hinterberger M, Steinert M, Koser S, Pinto S, et al. Thymic B cells Are licensed to present self antigens for central T cell tolerance induction. Immunity. 2015;42:1048–61. https://doi.org/10.1016/j.immuni.2015.05.013.
- 42. Xiao X, Qin S, Cui T, Liu J, Wu Y, Zhong Y, et al. Bacillus licheniformis suppresses Clostridium perfringens infection via modulating inflammatory response, antioxidant status, inflammasome activation and microbial homeostasis in broilers. Poult Sci. 2024;103:104222. https://doi.org/10.1016/j.psj.2024.104222.

- 43. Chen C, Wu L, Wang L, Tang X. Probiotics combined with budesonide and ipratropium bromide for chronic obstructive pulmonary disease: a retrospective analysis. Medicine (Baltimore). 2024;103:e37309. https://doi.https://doi.org/10.1097/MD.0000000000037309.
- 44. Shi H, Li X, Hou C, Chen L, Zhang Y, Li J. Effects of pomegranate peel polyphenols combined with inulin on gut microbiota and serum metabolites of high-fat-induced obesity rats. J Agric Food Chem. 2023;71:5733–44. https://doi.org/10.1021/acs.jafc.3c01014.
- 45. Singh RS, Vidhyasagar V, Yang S, Arna AB, Yadav M, Aggarwal A, et al. DDX41 is required for cGAS-STING activation against DNA virus infection. Cell Rep. 2022;39:110856, DOI: 10.1016/j.celrep.2022.110856.
- 46. Rothhammer V, Mascanfroni ID, Bunse L, Takenaka MC, Kenison JE, Mayo L, et al. Type I interferons and microbial metabolites of tryptophan modulate astrocyte activity and central nervous system inflammation via the aryl hydrocarbon receptor. Nat Med. 2016;22:586–97, DOI: 10.1038/nm.4106.
- 47. Agus A, Planchais J, Sokol H. Gut microbiota regulation of tryptophan metabolism in health and disease. Cell Host Microbe. 2018;23:716–24. https://doi.org/10.1016/j.chom.2018.05.003.
- 48. Tailford LE, Crost EH, Kavanaugh D, Juge N. Mucin glycan foraging in the human gut microbiome. Front Genet. 2015;6:81. https://doi.org/10.3389/fgene.2015.00081.
- 49. Youm YH, Nguyen KY, Grant RW, Goldberg EL, Bodogai M, Kim D, et al. The ketone metabolite β-hydroxybutyrate blocks NLRP3 inflammasome-mediated inflammatory disease. Nat Med. 2015;21:263–9, DOI: 10.1038/nm.3804.
- 50. Pham N, Chirayath TW, Castelli F, Fenaille F, Nguyen AL, Brial F, et al. POS0510 intermittent fasting reduces crystal-induced inflammation. Ann Rheum Dis. 2023;82. https://doi.org/10.1136/annrheumdis-2023-eular.5106.
- 51. Mao J, Xia W, Wu Y, Li M, Zhao Y, Zhai P, et al. Biosynthesis of Lysosomally Escaped Apoptotic Bodies Inhibits Inflammasome Synthesis in Macrophages. Research (Wash D C). 2025;8:0581. https://doi.org/10.34133/research.0581.
- 52. Gharib SA, McMahan RS, Eddy WE, Long ME, Parks WC, Aitken ML, et al. Transcriptional and functional diversity of human macrophage repolarization. J Allergy Clin Immunol. 2019;143:1536–48. https://doi.org/10.1016/j.jaci.2018.10.046.

53. Xia T, Zhang M, Lei W, Yang R, Fu S, Fan Z, et al. Advances in the role of STAT3 in macrophage polarization. Front Immunol. 2023;14:1160719. https://doi.org/10.3389/fimmu.2023.1160719.